Journal of Molecular Graphics and Modelling 38 (2012) 419–429

Contents lists available at SciVerse ScienceDirect

Journal of Molecular Graphics and Modelling

journal homepage: www.elsevier.com/locate/JMGM

Electronic structures and optical properties of organic dye sensitizer NKX derivatives for solar cells: A theoretical approach

Cai-Rong Zhang[a,b,*], Li Liu[a], Zi-Jiang Liu[c,d], Yu-Lin Shen[e], Yi-Tong Sun[e], You-Zhi Wu[b], Yu-Hong Chen[a,b], Li-Hua Yuan[a], Wei Wang[a], Hong-Shan Chen[f]

[a] Department of Applied Physics, Lanzhou University of Technology, Lanzhou, Gansu 730050, China
[b] State Key Laboratory of Gansu Advanced Non-ferrous Metal Materials, Lanzhou University of Technology, Lanzhou 730050, China
[c] Institute of Electronic Information Science and Technology, Lanzhou City University, Lanzhou 730070, China
[d] Institute of Applied Physics and Computational Mathematics, Beijing 100088, China
[e] Gansu Computing Center, Lanzhou 730000, China
[f] College of Physics and Electronic Engineering, Northwest Normal University, Lanzhou, Gansu 730070, China

ARTICLE INFO

Article history:
Received 2 June 2012
Received in revised form
12 September 2012
Accepted 15 September 2012
Available online 25 September 2012

Keywords:
Organic dye sensitizer
Electronic structure
Density functional theory
Absorption spectra
Dye sensitized solar cells

ABSTRACT

The photon to current conversion efficiency of dye-sensitized solar cells (DSCs) can be significantly affected by dye sensitizers. The design of novel dye sensitizers with good performance in DSCs depend on the dye's information about electronic structures and optical properties. Here, the geometries, electronic structures, as well as the dipole moments and polarizabilities of organic dye sensitizers C343 and 20 kinds of NKX derivatives were calculated using density functional theory (DFT), and the computations of the time dependent DFT with different functionals were performed to explore the electronic absorption properties. Based upon the calculated results and the reported experimental work, we analyzed the role of different conjugate bridges, chromophores, and electron acceptor groups in tuning the geometries, electronic structures, optical properties of dye sensitizers, and the effects on the parameters of DSCs were also investigated.

1. Introduction

The dye-sensitized nanocrystalline solar cell (DSC), which was presented by O'Regan and Gräzel [1], has attracted much attention because of easy fabrication, lower cost, and relatively higher photon to current conversion efficiency (PCCE) [2–5]. The typical DSC usually contain three important parts [4]: (i) the mesoporous oxide semiconductor nanoparticle layers, that were used as a part of photon-anode; (ii) dye sensitizers, that attached to the surfaces of the oxide semiconductors; (iii) electrolyte, that is the medium containing redox system, such as the iodide/triiodide couple. The photon to current conversion mechanism of DSC can be described as followings [4]: the photon absorptions of dye sensitizer result in the electron injection from the excited dyes to the conduction band of semiconductor nano-films; the oxidized dye sensitizer is subsequently reduced by electron transfer from the electrolyte; and the oxidized molecules of electrolyte is regenerated in turn by the reduction at the electrode.

Dye sensitizer has a significant influence on the PCCE [6–11]. Up to now, numerous dye sensitizers were designed, synthesized and characterized in order to improve the PCCE of DSC. Unfortunately, only several kinds of dye sensitizers have good performance. In metal–organic complexes, especially the noble metal ruthenium polypyridyl complexes, it was proved that the N3 and black dyes were the best dye sensitizers because the overall energy conversion efficiency is greater than 10% under air mass (AM) 1.5 irradiation [12–14]. On the other hand, metal-free organic dyes sensitizers, including cyanines [15–17], hemicyanines [18,19], triphenylmethanes [8,20,21], perylenes [22–26], coumarins [27–29], porphyrins [30–35], squaraines [36–38], indoline [39,40], and azulene-based dyes [41], were developed because of their high molar absorption coefficient, relatively simple synthetic procedure, various structures and lower cost. Recently, more than 10% PCCE of DSC has been achieved by using organic sensitizer C219 that contain ethylenedioxythiophene and dithienosilole blocks [42]. So, the development of novel organic dye sensitizer is a promising way to improve the PCCE of DSC.

* Corresponding author at: Department of Applied Physics, Lanzhou University of Technology, Lanzhou, Gansu 730050, China. Tel.: +86 0931 2973780; fax: +86 0931 2976040.
E-mail address: zhcrxy@lut.cn (C.-R. Zhang).

1093-3263/$ – see front matter © 2012 Elsevier Inc. All rights reserved.
http://dx.doi.org/10.1016/j.jmgm.2012.09.004

Since the electron injection from the coumarin 343 (C343) to the conduction band of TiO_2 was reported [43], coumarin dye derivatives had been recognized as effective dye sensitizers for DSC. However, the PCCE of C343 sensitized DSC is much lower than that of Ru complex sensitizer because of narrow effective absorption region of C343. To achieve higher PCCE, the wide absorption band in visible region is expected. Generally, the metal-free organic dye sensitizer has typical donor π-conjugate bridge acceptor (D-π-A) structure. One of the approaches to improve the harvest of solar energy is elongating the π-conjugate bridge [44]. According to this clue, the dye sensitizers NKX-2311, etc. were synthesized [27,44–46], and the 5.6% PCCE was achieved by NKX-2311 sensitized DSC [44,46]. Furthermore, the introducing π-conjugate ring moieties (benzene, thiophene, pyrrole, and furan) into the methane chain of NKX-2311 extend π-conjugation, and contribute to a red-shift in the absorption spectrum, also increase the stability of the dye molecules [46–51]. Alternatively, using different chromophores can tune the electronic and optical properties of dye sensitizers [27,52,53], and then affect on the PCCE. For instance, the 5.9% PCCE was achieved by using dye sensitizer NKX-2600, which bear strong electron donating *N*,*N*-dimethylaniline (DMA) moieties [53]. Also, the different electron acceptor groups, such as cyanoacetic acid (CAA) moiety, carboxyl group, and rhodanine acetic acid (RAA) group, can change withdrawing electron abilities and optical properties in dye sensitizer [27]. The substitution of chromophores, conjugate bridges, and electron acceptor groups are effective methods to tune the electronic and optical properties of dye sensitizers.

Further developments of novel dye sensitizer depend on the quantitative knowledge of dye sensitizers [9,11,54]. The theoretical investigations of the physical properties of dye sensitizers are very important to disclose the relationships among the performance, structures and the properties. For instance, on the basis of density functional theory (DFT) calculations for the chemical structures and exciton binding energies of several pure organic dyes, the novel organic triphenylamine-based dye sensitizer EB-01 was designed, and the over 9% of PCCE was achieved by EB-01 sensitized DSC [55]. For NKX derivatives (C343, NKX-2398, NKX-2388, NKX-2384, NKX-2311, NKX-2510, NKX-2586, NKX-2393, NKX-2460, NKX-2475, NKX-2195), the B3LYP/3-21G* molecular orbital (MO) calculations of the ground states indicated that the highest occupied MO (HOMO) localized in coumarin framework, and the lowest unoccupied MO (LUMO) extended from carboxyl to —CH=CH— unit in conjugate bridge. Thus, it was deduced that electron can transfer from coumarin framework to carboxyl and —CH=CH— unit during photo-excitation [27]. The absorption spectra of several coumarin derivative dyes (C343, NKX-2388, NKX-2311, NKX-2586, NKX-2677) were investigated by using configuration interaction singles (CIS), time dependent DFT (TDDFT, B3LYP/6-31G(d,p)), and coupled cluster singles and doubles (CISD) method [56]. The electronic structure and absorption spectra of a couple of coumarin dye sensitizers (C343, NKX-2398, NKX-2388, NKX-2311, NKX-2586) were calculated using DFT and TDDFT (B3LYP/6-31G(d)), and they also analyzed why the NKX-2311 dye has good performance in DSC [57]. The properties of the ground and excited states, as well as the effects of electric field of the dye sensitizer NKX-2807 were reported by Hashemianzadeh et al. [58] In this work, in terms of experimental synthesized dye sensitizer NKX derivatives, the electronic structure and optical absorption properties of 21 dye sensitizers (see Figs. 1–6) were calculated by using DFT and TDDFT. Based upon the calculated results, we analyzed the role of different conjugate bridges, chromophores, and electron acceptor groups in tuning the geometries, electronic structures and optical properties. Also, we further investigated the effects of the conjugate bridges, chromophores, and electron acceptor groups in the parameters of DSC.

2. Computational methods

The geometries, electronic structures, as well as dipole moments and polarizabilities for dye sensitizer C343 and NKX derivatives were calculated using DFT B3LYP [59–61] functional with Gaussian03 package [62]. The comparison with MP2 geometries of several dye molecules confirmed the accuracy of B3LYP for the geometry optimizations [63]. All calculations were performed without any symmetry constraints with the polarized split-valence 6-31G* basis sets. For the electronic absorption spectra, it requires the calculations of allowed excitations and oscillator strengths. These calculations were carried out using TDDFT method in gas phase and solvent. Generally, for the dye sensitizers with good performance in DSC, the electronic excitations are charge transfer (CT) processes. To obtain better description of CT excited states, the different exchange-correlation functionals (B3LYP, PBE0 [64], and long-range-corrected hybrid functional LC-wPBE [65–68]) and basis sets (6-31G*, 6-31G(d,p), and 6-31 + G(d,p)) were adopted for calculating electronic absorption spectra. The TDDFT calculations with LC-wPBE functional were performed by using Gaussian09 package [69]. The non-equilibrium version of the polarizable continuum model (PCM) [70] was adopted for considering the solvent effects. The UV–vis spectra were simulated via SWizard program [71], and assuming each transition is Gaussian distribution with full width at half-maximum (fwhm) of 3000 cm^{-1}.

3. Results and discussion

The coumarin 343 (C343) is basic model, and the optimized structure is presented in Fig. 1. In order to investigate the role of different conjugate bridges, chromophores, and electron acceptor groups in tuning the geometries, electronic structures and optical properties, the dye sensitizer NKX derivatives were classified into different groups. In the group 1 (G1, including NKX-2311, NKX-2388, NKX-2587, NKX-2593, NKX-2586, NKX-2677, NKX-2697, NKX-2700, NKX-2753), the electron donors and acceptors are coumarin and CAA moieties, respectively. Though NKX-2807 and NKX-2883 have the same donor and acceptor moieties of G1, they were selected to construct G2 because their conjugate bridges have strong electron pull group —CN. The electron donor and acceptor in group 3 (G3, including NKX-2554, NKX-2569, and NKX-2600) are DMA and CAA moieties, respectively. Only the conjugate bridges are different in each group. The group 4 (G4, including NKX-2311 and NKX-2393) and the group 5 (G5 including NKX-2195 and NKX-2398) contain different electron acceptor moieties in each group. The group 6 (G6, including NKX-2510, NKX-2311 and NKX-2553) and the group 7 (G7, including NKX-2384 and NKX-2388) possess different chromophores in donor parts of dyes. The optimized structures of the dyes are shown in Figs. 2–6.

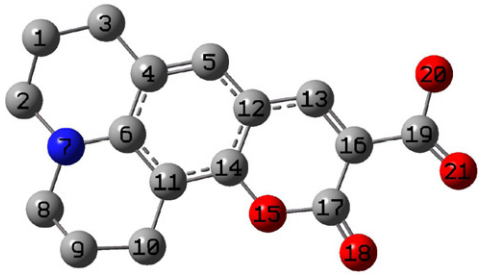

Fig. 1. The optimized geometrical structures of the dye molecule C343 with atomic serial numbers. (Hydrogen atoms have been omitted for clarity, gray circles: C, blue circles: N, red circles: O.)

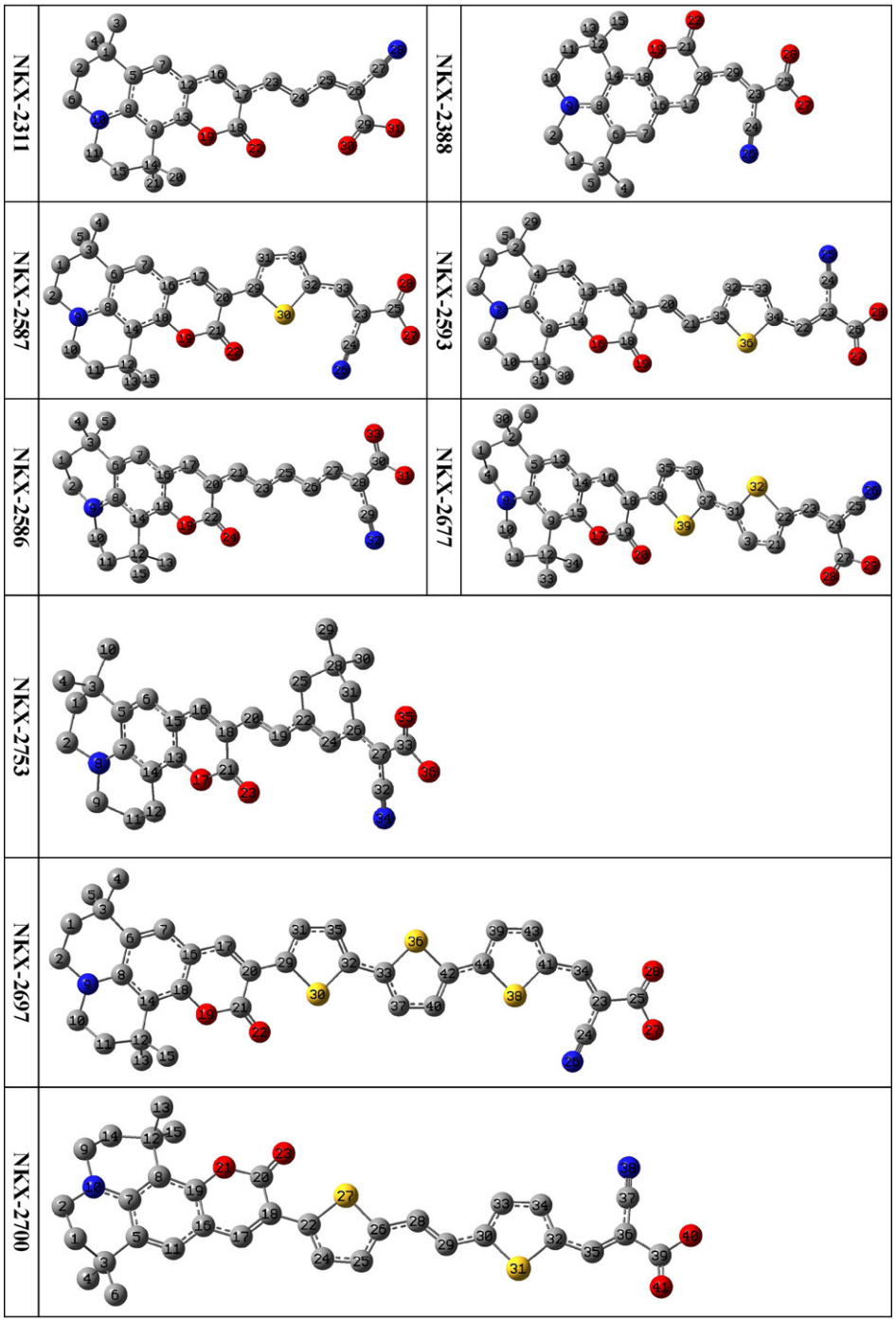

Fig. 2. The optimized geometrical structures of the dye molecules in group 1 (G1) with atomic serial numbers. (Hydrogen atoms have been omitted for clarity, gray circles: C, blue circles: N, red circles: O; yellow circles: S.) (For interpretation of the references to color in this figure caption, the reader is referred to the web version of the article.)

3.1. The geometric structures

The geometrical parameters of NKX-2311 were presented in the published works by Hara et al. [27] and Kurashige et al. [56]. The corresponding values of the geometry agree well with that of present work. In terms of the calculated data, the geometric parameters of same group (coumarin framework, DMA, CAA, etc.) in different dyes are very similar because of the localized interaction in chemical bonds. The calculated geometries indicate that the conjugate bridges of NKX-2554, NKX-2569, and NKX-2600 are not coplanar with the DMA moieties. The torsion angles between carboxyl groups and conjugate bridges in NKX-2195, NKX-2384, and NKX-2393 dyes are about 84°, 4°, and 35/15° (NKX-2393 have 2 —COOH groups), respectively. This is resulted from steric hindrance effects. The experimental PCCE (2.6%, 3.1%, 3.7%) and open circuit voltage (V_{oc}, 0.49 V, 0.50 V, 0.48 V) of NKX-2195, NKX-2384, and NKX-2393 dyes are lower [27,52,53]. For the other NKX derivatives, the carboxyl and the framework of coumarin are coplanar with the different bridge groups. These geometric characters are listed in Table 1. The planar conjugated effects extend the delocalization of electron, and thus it is helpful for efficient CT from the chromophore to the carboxyl group. Similar geometric characters

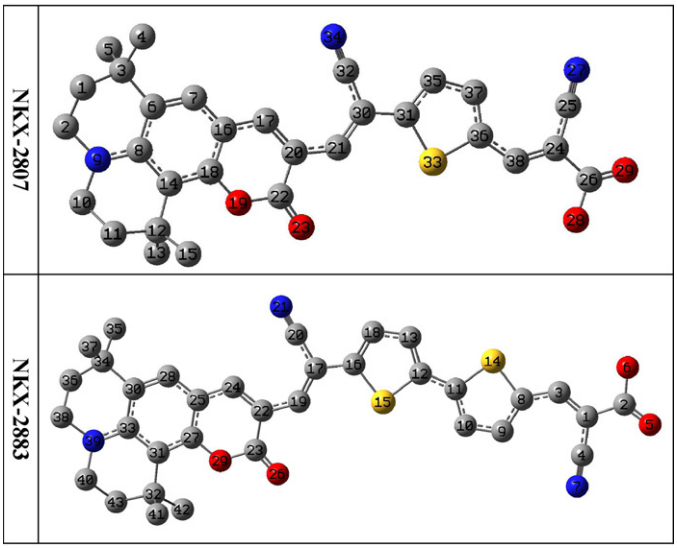

Fig. 3. The optimized geometrical structures of the dye molecules in group 2 (G2) with atomic serial numbers. (Hydrogen atoms have been omitted for clarity, gray circles: C, blue circles: N, red circles: O; yellow circles: S.) (For interpretation of the references to color in this figure caption, the reader is referred to the web version of the article.)

are also appeared in the organic dye sensitizers JK-1 and JK-2 [72], JK-16 and JK-17 [73,74], and other organic dyes which contain CAA group [75–78].

Furthermore, in order to describe the length of conjugate bridge of the dyes, we define "*L*" as the distance between two special C atoms. The one is C atom in carboxyl group. The other one is the C atom that connects the conjugate bridge and the donor groups. When the dyes adsorbed on the surface of semiconductor nanoparticles, the *L* can describe the length of CT that occurred at the interface between dyes and semiconductor nanoparticles, and also can describe conjugate length in some extent. On the basis

Table 1
The calculated *L* of the dyes C343 and NKX derivatives.

Dyes	*L*[a]/nm	Coplanarity?[b]	Coplanarity?[c]
C343	0.1480	Y	Y
NKX-2195	0.6567	Y	N
NKX-2311	0.5559	Y	Y
NKX-2384	0.3855	Y	N
NKX-2388	0.3846	Y	Y
NKX-2393	0.6218	Y	N
NKX-2398	0.3831	Y	Y
NKX-2510	0.6256	Y	Y
NKX-2553	0.6314	Y	Y
NKX-2554	0.4943	N	Y
NKX-2569	0.7388	N	Y
NKX-2600	0.8933	N	Y
NKX-2587	0.7605	Y	Y
NKX-2593	1.0186	Y	Y
NKX-2586	0.8701	Y	Y
NKX-2677	1.0864	Y	Y
NKX-2697	1.5400	Y	Y
NKX-2700	1.4116	Y	Y
NKX-2753	0.8778	Y	Y
NKX-2807	0.9771	Y	Y
NKX-2883	1.3682	Y	Y

[a] *L* is the distance between the C atom in carboxyl group and the other C atom which connected with conjugate bridge.
[b] Is the conjugate bridge coplanar with the framework of coumarin or the *N*,*N*-dimethylaniline (DMA) moiety?
[c] Is the conjugate bridge coplanar with the carboxyl group?

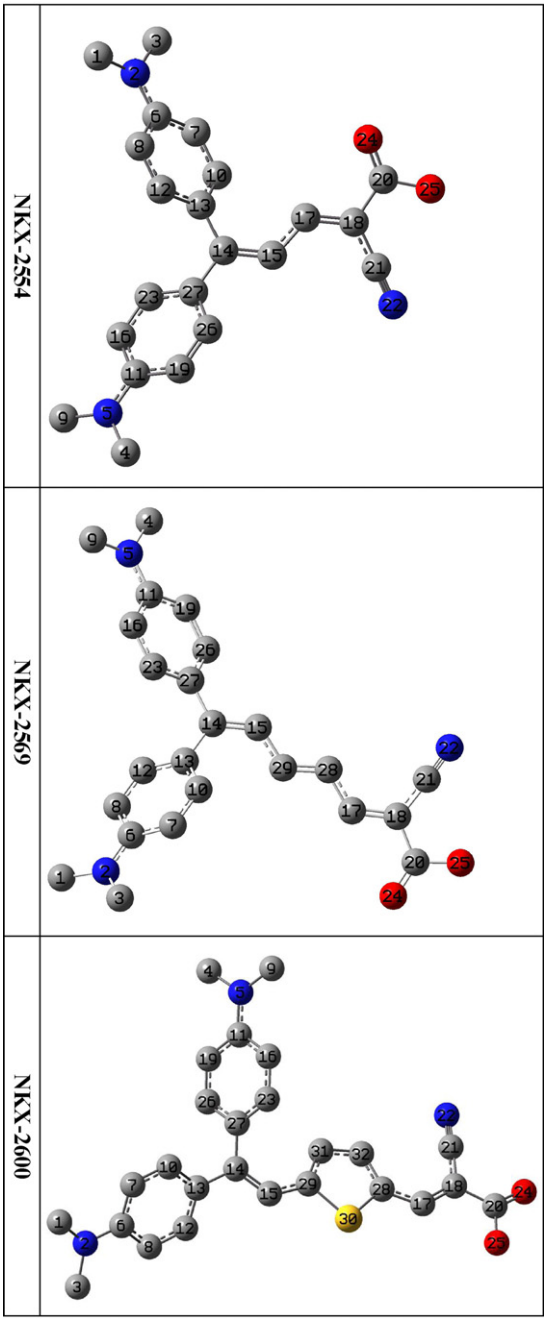

Fig. 4. The optimized geometrical structures of the dye molecules in group 3 (G3) with atomic serial numbers. (Hydrogen atoms have been omitted for clarity, gray circles: C, blue circles: N, red circles: O; yellow circles: S.) (For interpretation of the references to color in this figure caption, the reader is referred to the web version of the article.)

of the calculated *L* and the reported photovoltaic experimental data [27,47,50,52,53], the following properties could be found: the shorter *L* (C343, NKX-2384, NKX-2388, and NKX-2398) is not favorable to improve the dye performance in DSC due to their lower PCCE (0.9%, 3.1%, 4.1%, 3.4%, respectively), this may be resulted from the shorter *L* could not generate effective charge separated states by photo excitation; but the moderate PCCE 6.4% of NKX-2697, which has the longest *L*, suggests that the longest *L* is also unfavorable to improve PCCE. It is understandable because the longer *L* may increases the possibility that the excited electrons can decay from the dye's donor group to the electrolyte. So, *L* is also a key parameter for optimizing dye sensitizers.

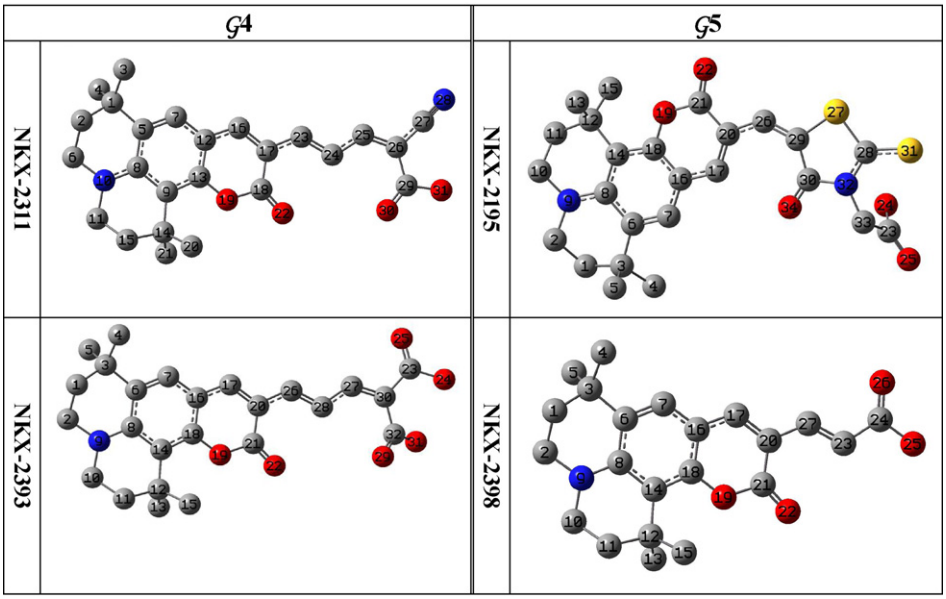

Fig. 5. The optimized geometrical structures of the dye molecules in groups 4 (G4) and 5 (G5) with atomic serial numbers. (Hydrogen atoms have been omitted for clarity, gray circles: C, blue circles: N, red circles: O; yellow circles: S.) (For interpretation of the references to color in this figure caption, the reader is referred to the web version of the article.)

3.2. Electronic populations

Natural Bond Orbital (NBO) calculations were performed in order to analyze the charge populations of the NKX derivatives and C343. The electron donor units of the dyes in this work are the coumarin, DMA, and other moieties. The electronic acceptors are CAA, carboxylate (C343, NKX-2398), and double carboxylate (NKX-2393). The calculated natural charges that populated in the electron donor, conjugate bridge, and electron acceptor groups are listed in Table 2. Totally, CAA is a strong electronic pull group. The data also suggest the charges of similar acceptors in different dyes are very similar, but the charges of donors and conjugate bridges are more flexible. This means that the natural charges in dye sensitizers are dominated by acceptor moieties. In G1 ∼ G3, the different conjugate bridges slightly affect on charge populations, but the thienyl in bridges also donate electrons to acceptor group. So, the thienyl-based bridges have double role, one is conjugate bridge to enhance the electronic delocalization, and the other is a part of electron donor. Furthermore, the thienyl groups in conjugate bridges shorten the distance of charge centers between positive and negative, and then reduce dipole moment. This is proved by the data of Section 3.4. Compared with NKX-2311, double carboxyl groups in NKX-2393 generate little charges in acceptor and negative charges in coumarin group because of its weaker pull electron ability, and thus the dipole of NKX-2393 has the opposite direction of other dyes. In G5, the charges of rhodanine ring are −0.48 *e* in NKX-2195, and introducing rhodanine significantly increase the charges of donor and bridge because the acceptor moiety rhodanine is strong electron pull group. In G6, the different chromophores slightly affects on the electronic populations in acceptors of dyes. As to G7, introducing —CF_3 reduce the charges of acceptor and donor.

Table 2
The calculated natural charges of electron donor, conjugate bridge, and electron acceptor groups for the C343 and NKX derivatives.

Dye	Donor	Acceptor	Bridge
C343	0.004	−0.004	
NKX-2311	0.073	−0.314	0.241
NKX-2587	0.063	−0.323	0.260
NKX-2593	0.029	−0.332	0.303
NKX-2586	0.049	−0.325	0.276
NKX-2677	0.036	−0.334	0.298
NKX-2697	0.021	−0.328	0.307
NKX-2700	0.034	−0.336	0.302
NKX-2753	0.031	−0.333	0.302
NKX-2807	0.111	−0.287	0.176
NKX-2883	0.090	−0.293	0.203
NKX-2554	0.253	−0.377	0.124
NKX-2569	0.206	−0.369	0.163
NKX-2600	0.165	−0.341	0.176
NKX-2393	−0.275	−0.009	0.284
NKX-2195	0.111	0.038	−0.149
NKX-2398	0.032	−0.051	0.019
NKX-2510	0.064	−0.308	0.244
NKX-2553	0.128	−0.332	0.204
NKX-2384	0.032	−0.244	0.212
NKX-2388	0.122	−0.330	0.208

When the dyes adsorbed on the surface of titanium dioxides, the electric potential barrier will be set up because of the negative charges of electron acceptor groups in dyes and the oxygen layer which is the terminal layer of oxides semiconductor surface. In general, the electromotive force (ε) of batteries related to a non-static electric field, which means the movement of electron from the battery cathode to the anode (forming a closed circuit) must input external energy to overcome this non-static electric field. The larger electric potential barrier will correspond to the larger non-static electric field, and then correspond to larger ε and V_{oc} for solar cells. The more charges populated in acceptor is favorable to increase V_{oc}. Both the data and fitted curve in Fig. 7 support the correctness of this tendency. Furthermore, when the dye molecule attach to the semiconductor surface, the strong electronic pull group in acceptor generate a larger electric filed, which can shift the conduction band edge (CBE) of semiconductor. Since the V_{oc} corresponds to the difference between the redox potential of electrolyte and CBE of semiconductor, the electronic pull group can tune the V_{oc} by meanings of shifting the CBE of semiconductor. So, introducing strong electronic pull group in acceptor of dye sensitizer is a possible way to increase V_{oc} of DSC.

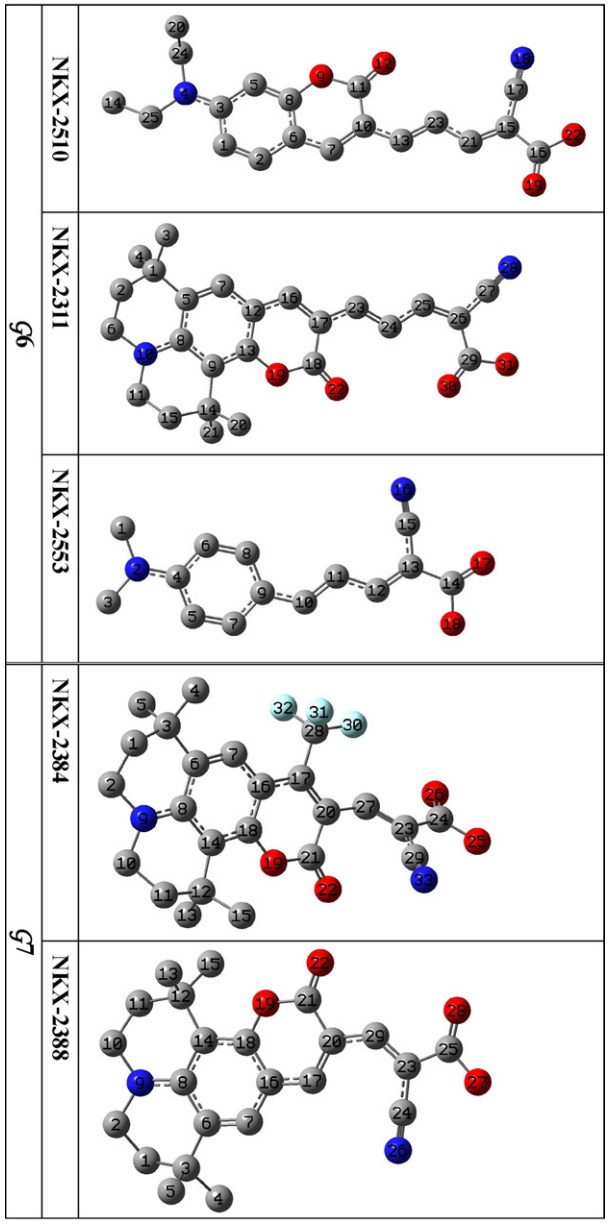

Fig. 6. The optimized geometrical structures of the dye molecules in groups 6 (G6) and 7 (G7) with atomic serial numbers. (Hydrogen atoms have been omitted for clarity, gray circles: C, blue circles: N, red circles: O; yellow circles: S; cyan circles: F.) (For interpretation of the references to color in this figure caption, the reader is referred to the web version of the article.)

3.3. Energy level alignment

The HOMO level corresponds to the oxidation potential of dye sensitizer [13], and the larger oxidation potential increase the driving force for the reduction of oxidized dye [56]. The HOMO and LUMO energies, as well as the HOMO–LUMO gaps (E_g) of C343 and NKX derivatives in gas phase and solvent are listed in Table 3. Solvent effects increase the HOMO of the dyes except NKX-2554, NKX-2569, and NKX-2600, and stabilize the LUMO of the dyes. Thus, compared with the data in gas phase, solvent effect reduces the E_g of these dyes. The driving force for the reduction of the oxidized NKX-2384 may be slightly larger than that of other dyes because of its lowest HOMO level. In G1, the increasing length of alkyl and thiophene chain can destabilize the HOMO and reduce the E_g. While in G2, due to the electron rich character of thiophene, the

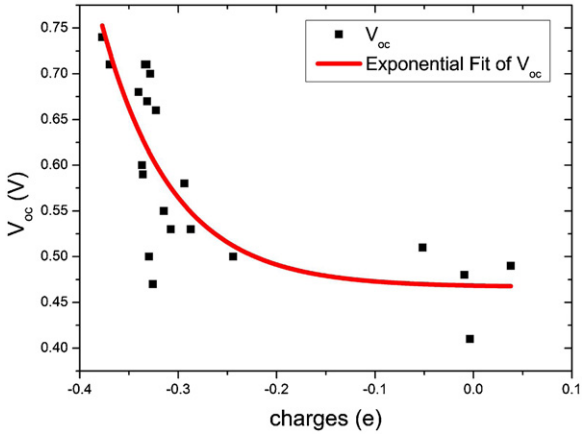

Fig. 7. The open-circuit voltage V_{oc} versus the charges of acceptor groups in C343 and NKX derivatives.

substituting bithienyl for thienyl can increase the HOMO and LUMO, and decrease the E_g about 0.12 eV and 0.08 eV in gas phase and in solvent, respectively. For G3, the increasing of alkyl length and the substituting thienyl for ethylene generate similar results in G1. The above tendency indicate that the longer alkenyl and thiophene chain in conjugate bridge result in higher HOMO, and then induce smaller driving force for the reduction of oxidized dyes. As to G4 and G5, substituting cyanoacrylic acid for double carboxyl group and introducing pull-electron group rhodanine ring stabilize the HOMO and LUMO, and reduce the E_g, and then the substitution can increase driving force for the reduction of the oxidized dyes. The substitution and introducing rhodanine ring in acceptor group are energetically favorable for the regeneration of oxidized dyes. In G6, coumarin group generates the smallest E_g (2.67 eV in solvent), which means the absorption of the dye with coumarin group has red shift relative to that of other dyes based upon single electron approxiamtion. In G7, introducing $-CF_3$ in chromophore stabilize the HOMO and LUMO, and decrease the E_g about 0.11 eV in solvent. But, because the change of E_g by introducing $-CF_3$ is more significant than that on HOMO energy, the influence of introducing of $-CF_3$ on absorption properties are much larger than that on driving force.

Table 3
The frontier molecular orbitals (MO) energies and HOMO–LUMO gaps (E_g) of C343 and NKX derivatives (in eV).

Dye	Gas phase			Solvent		
	HOMO	LUMO	E_g	HOMO	LUMO	E_g
C343	−5.46	−1.89	3.57	−5.38	−1.97	3.41
NKX-2195	−5.41	−2.68	2.83	−5.35	−2.76	2.59
NKX-2311	−5.41	−2.61	2.80	−5.29	−2.62	2.67
NKX-2384	−5.65	−2.73	2.92	−5.51	−2.83	2.68
NKX-2388	−5.57	−2.61	2.96	−5.49	−2.70	2.79
NKX-2393	−5.27	−2.34	2.93	−5.22	−2.42	2.80
NKX-2398	−5.32	−2.00	3.32	−5.25	−2.05	3.20
NKX-2510	−5.56	−2.64	2.92	−5.44	−2.66	2.78
NKX-2553	−5.40	−2.34	3.06	−5.29	−2.40	2.89
NKX-2554	−5.07	−2.08	2.99	−5.19	−2.35	2.84
NKX-2569	−4.95	−2.30	2.65	−5.00	−2.50	2.50
NKX-2586	−5.29	−2.68	2.61	−5.17	−2.70	2.47
NKX-2587	−5.28	−2.54	2.74	−5.21	−2.64	2.57
NKX-2593	−5.20	−2.65	2.55	−5.08	−2.72	2.36
NKX-2600	−4.87	−2.37	2.50	−4.89	−2.60	2.29
NKX-2677	−5.14	−2.67	2.47	−5.04	−2.76	2.28
NKX-2697	−4.96	−2.68	2.28	−4.92	−2.80	2.12
NKX-2700	−4.96	−2.66	2.30	−4.87	−2.76	2.11
NKX-2753	−5.19	−2.53	2.66	−5.14	−2.63	2.51
NKX-2807	−5.47	−3.03	2.44	−5.33	−3.05	2.28
NKX-2883	−5.29	−2.97	2.32	−5.18	−2.98	2.20

Table 4
The dipole moments μ and the isotropic polarizabilities α of C343 and NKX derivatives.

Dyes	μ (a.u.)	α (a.u.)
C343	3.77	210.18
NKX-2195	4.67	432.67
NKX-2311	5.42	407.99
NKX-2384	3.33	321.83
NKX-2388	3.80	325.19
NKX-2393	3.88	397.31
NKX-2398	3.42	301.47
NKX-2510	5.24	340.49
NKX-2553	4.30	240.07
NKX-2554	3.82	343.83
NKX-2569	4.68	424.88
NKX-2586	5.68	495.81
NKX-2587	5.10	447.58
NKX-2593	5.06	545.11
NKX-2600	4.66	467.20
NKX-2677	6.23	610.80
NKX-2697	5.76	751.73
NKX-2700	6.41	724.23
NKX-2753	5.30	506.92
NKX-2807	5.97	559.90
NKX-2883	5.54	705.92

The published HOMO and LUMO energies of the bare $Ti_{38}O_{76}$ cluster as a model for nanocrystalline are −6.55 and −2.77 eV respectively, resulting in a HOMO–LUMO gap of 3.78 eV, the lowest transition is reduced to 3.20 eV according to TDDFT, and this value is slightly smaller than typical band gap of TiO_2 nanoparticles [20]. Through the calculated HOMO, LUMO and E_g of C343, NKX derivatives and $Ti_{38}O_{76}$ cluster, we can find that the HOMO energy of C343 and NKX derivatives fall within the TiO_2 gap. These data reveal the sensitized mechanism: the interfacial electron transfer between semiconductor TiO_2 electrode and dye sensitizer NKX derivatives is electron injection (adiabatic and nonadiabatic) process from the excited dyes to the semiconductor conduction band.

3.4. Dipole moments and polarizabilities

Dipole and polarizability are very important physical quantities of dye sensitizer. Polarizabilities could determine not only the strength of molecular interactions, as well as the cross sections of different scattering and collision processes, but also the nonlinear optical properties (NLO) of the system [79]. It has been reported that hemicyanine dye sensitizer, which has prominent NLO property, usually possesses good photoelectric conversion efficiency [80]. Our previous theoretical studies of several organic dye sensitizers indicated that the dyes with larger the isotropic polarizability α usually correspond to larger extent of electron delocalization and insufficient charge separation in excited CT states [75]. In order to investigate the relationships among PCCE, the dipole moments and polarizabilities, these quantities of C343 and NKX derivatives were calculated. The following formula was adopted to calculate the dipole moment μ,

$$\mu = \sqrt{\mu_x^2 + \mu_y^2 + \mu_z^2},$$

where μ_x, μ_y, μ_z are vector components of dipole moment. The definitions of the isotropic polarizability α were presented by Christiansen et al. [79],

$$\alpha = \frac{1}{3}(\alpha_{XX} + \alpha_{YY} + \alpha_{ZZ}),$$

where α_{xx}, α_{yy}, α_{zz} are tensor components of polarizability. The results are listed in Table 4. Interestingly, we can find a general tendency that the dyes with larger polarizabilities usually possess the larger dipole moments. This resulted from that the longer conjugate bridge enhances the electronic delocalization.

For G1 ~ G3, elongating of alkenyl conjugate bridge increases μ and α, and substituting oligothiophene for thienyl increase α and decrease μ. The longer alkenyl and oligothiophene enhance the delocalization of electron in conjugate bridge, and thus induce the increasing of α. In G4 and G5, the strong electron pull group in the acceptor increases the dipole moment μ and the isotropic polarizability α. In G6, the μ and α increase in the order of NKX-2553, NKX-2510, and NKX-2311. Only the donor parts among these dyes are different. The donor part of NKX-2311 is more delocalized than that of others because of its multi-ring structure. For G7, compared to NKX-2388, introducing $-CF_3$ in coumarin (NKX-2384) decreases μ and α of the dye because the pull-electron group $-CF_3$ induce localization of electron in the donor part of dye.

Dipolar field that exerted on the TiO_2 surface by dye sensitizers induce the shift conduction bands [81], and then affect on the photovoltages. The dipole moment points from negative to positive charge. The dipoles point away from the surface when the D-π-A organic dyes adsorbed on the TiO_2 nanoparticles. An up shift of the valence and conduction band was induced by this kind of dipole fields [81]. In terms of that calculated dipoles of these dyes, elongating the conjugate bridge using alkenyl and introducing strong pull electron group in the acceptor can tune the up-shift of valence and conduction bands of TiO_2, and thus affect on the V_{oc} of DSC, while the effect of elongating thienyl-based conjugate bridge is smaller because of smaller dipole moments.

3.5. Optical absorption properties

Up to now, in the framework of TDDFT, there is not a density functional that can describe excitation very well for any system, and the error of a functional depends on system. For instance, the appropriate functional for triphenylamine dyes are BhandH [82–84]. However, based upon TDDFT calculations for 5 representative dyes (L0, D4, D5, C217, and JK2), Pastore et al. reported that the MPW1K and CAM-B3LYP functionals represent a valuable tool of comparable accuracy to that of high level ab initio methods [63]. Nowadays, for a giving system, the suitable functional for describing CT excitations is long range corrected (LRC) hybrid functional with optimized range-separation parameter [85]. But we should adopt different parameter for different systems because the optimized range-separation parameter, which may be related to the extent of electron delocalization, depends on

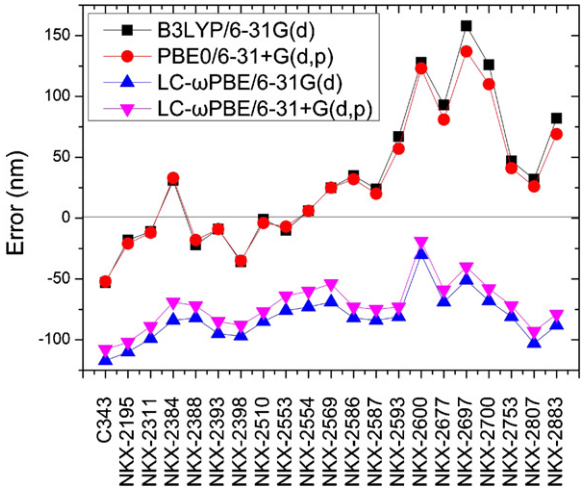

Fig. 8. The calculated λ_{max} error of the dye molecules C343 and NKX derivatives from different functionals and basis sets.

Table 5
The calculated excitation energies (eV), wavelength (nm), electronic transition configurations, oscillator strengths (f) and the short circuit photocurrent density J_{sc} (mA/cm^2) for the singlet → singlet transitions of the absorption band in visible and ultraviolet region for C343 and NKX derivatives in solvent.

Dyes	Excited states	Assignment (only the configurations composition larger than 10% were listed)	E (eV/nm)	f	J_{sc} [a]
C343	1	H → L (84%)	3.18/390	0.6392	4.1
NKX-2195	1	H → L (82%)	2.39/518	1.2547	7.5
	5	H → L + 1 (42%); H-1 → L (35%)	3.56/348	0.1127	
NKX-2311	1	H → L (83%)	2.51/495	1.5531	15.2
	3	H → L + 1 (76%); H-2 → L (17%)	3.58/346	0.1254	
	4	H-2 → L (60%); H-1 → L (10%)	3.83/323	0.2630	
NKX-2384	1	H → L (82%)	2.43/510	0.6865	9.4
NKX-2388	1	H → L (79%)	2.61/475	1.0571	12.9
NKX-2393	1	H → L (83%)	2.60/477	1.4987	12.8
	4	H-2 → L (62%); H-1 → L (14%)	3.89/318	0.2767	
NKX-2398	1	H → L (83%)	2.98/416	1.0819	11.1
NKX-2510	1	H → L (83%)	2.60/476	1.6176	13.2
	4	H-1 → L (46%); H-2 → L (30%)	3.90/318	0.2073	
NKX-2553	1	H → L (80%)	2.76/450	1.3762	10.4
NKX-2554	1	H → L (51%); H-1 → L (37%)	2.55/486	0.4500	9.9
	2	H-1 → L (54%); H → L (32%)	2.66/466	0.7908	
	4	H-2 → L (75%)	4.02/309	0.2400	
NKX-2569	1	H → L (76%)	2.29/541	1.0368	12.9
	2	H-1 → L (86%)	2.49/497	0.5361	
	3	H-2 → L (83%)	3.57/347	0.3669	
NKX-2586	1	H → L (83%)	2.30/538	1.8746	15.1
	2	H → L + 1 (46%); H-1 → L (42%)	3.27/380	0.3595	
	4	H-1 → L (41%); H → L + 1 (34%)	3.52/353	0.1260	
NKX-2587	1	H → L (85%)	2.35/527	1.3844	12.1
	2	H → L + 1 (70%); H-1 → L (24%)	3.24/382	0.1799	
	4	H-1 → L (46%); H-2 → L (25%)	3.50/354	0.1021	
NKX-2593	1	H → L (86%)	2.19/567	1.6590	14.89
	2	H-1 → L (48%); H → L + 1 (46%)	3.06/406	0.6054	
NKX-2600	1	H → L (83%)	2.07/598	0.9177	12.5
	2	H-1 → L (93%)	2.39/519	0.3356	
	3	H-2 → L (72%); H → L + 1 (22%)	3.22/385	0.3526	
	5	H-1 → L + 1 (92%)	3.75/330	0.2655	
NKX-2677	1	H → L (87%)	2.10/592	1.6310	13.5
	2	H → L + 1 (56%); H-1 → L (38%)	2.85/435	0.5890	
NKX-2697	1	H → L (87%)	1.94/638	1.6842	14.3
	2	H-1 → L (54%); H → L + 1 (38%)	2.62/474	0.7508	
	7	H-3 → L (58%); H-1 → L + 1 (12%); H → L + 2 (10%)	3.55/349	0.1003	
NKX-2700	1	H → L (86%)	1.95/635	1.9747	12.0
	2	H-1 → L (52%); H → L + 1 (41%)	2.69/462	0.7263	
NKX-2753	1	H → L (85%)	2.33/533	1.6652	16.1
	2	H → L + 1 (55%); H-1 → L (37%)	3.26/380	0.3952	
	4	H-1 → L (40%); H-2 → L (25%); H → L + 1 (16%)	3.48/356	0.1455	
NKX-2807	1	H → L (83%)	2.09/592	1.6556	10.93
	2	H → L + 1 (69%); H-1 → L (26%)	2.91/427	0.2040	
NKX-2883	1	H → L (85%)	2.00/621	1.8737	16.9
	2	H → L + 1 (75%); H-1 → L (18%)	2.61/476	0.3046	
	3	H-1 → L (68%); H → L + 1 (12%)	2.83/438	0.1810	
	7	H-3 → L (56%); H → L + 2 (15%); H-4 → L (10%)	3.72/334	0.1272	
	11	H → L + 3 (69%)	4.13/300	0.1653	

[a] The references of experimental J_{sc} are same to that in text.

the system under study. For a series of systems, we should calculate the structures and properties at the same theoretical method in order to compare them. To do that, the LC-wPBE with default range-separation parameter was selected as a representative LRC functional in the calculations. On the other hand, several references demonstrated that the PBE0 functional outperforms other global hybrid functionals in the computations of UV–vis spectra [86,87]. Also, the popular hybrid functional B3LYP was adopted for calculating structure and properties in many references. Furthermore, we focused on the relative band shifts of dye sensitizers with different conjugate bridges, chromophores, and electron acceptor groups, rather than in absolutely reproducing excitation energies. So, B3LYP, PBE0, and LC-ωPBE functionals were employed as representative functionals for calculating UV–vis spectra.

The electronic absorption λ_{max} values of experiment and different theoretical methods are listed in Table S1 in supporting information (SI). The simulated spectra are displayed in Table S2 in SI. The data indicates the results of TD-DFT with different methods have different extent of discrepancy between experimental and theoretical results. The discrepancy resulted from DFT exchange

and correlation functional and the computational model of solvent effects [75]. In order to see the dependence of computational error on theoretical methods clearly, Fig. 8 presents the error which was defined as theoretical λ_{max} minus experimental λ_{max}. It can be found that, for the dyes without thienyl group in conjugate bridge, most of the PBE0/6-31 + G(d,p) results agree well with that of experiment, but for the dyes with thienyl or polythiophenes in conjugate bridge, both PBE0/6-31 + G(d,p) and LC-ωPBE/6-31 + G(d,p) have to confront challenge. Further calculations are therefore needed to shed more light on the reproduce the experimental absorption properties of dye sensitizer with the thienyl or polythiophenes in conjugate bridge. The investigations toward this are in progress in our group. However, for most of the dyes, the λ_{max}, line shape and relative strength calculated using PBE0 are better than that of LC-ωPBE and B3LYP to agree with that of experiment. So, the results of TD-PBE0/6-31 + G(d,p) are adopted for analyzing the spectral features of these dyes.

To obtain the microscopic information about the electronic transitions, we check the corresponding MO properties. The absorption in visible and near-UV region is the most important region for photo to current conversion, so only the singlet → singlet transitions of the absorption bands with the wavelength longer than 300 nm and the oscillator strength larger than 0.1 are listed in Table 5. The isodensity plots of the frontier MOs that related to the absorption in visible and near-UV region are presented in Table S3 in SI. The HOMOs of these dyes mainly contributed from the donor and conjugate bridge parts, whereas the LUMOs mainly located on the acceptor and conjugate bridge groups. For these dyes, the maximum absorptions in UV/vis spectra approximately arise from HOMO → LUMO $\pi \rightarrow \pi^*$ transitions. Furthermore, the main overlap between HOMO and LUMO of the dyes suggest the maximum absorptions have some local excited transitions in conjugate bridge. While the relocations of the HOMOs and LUMOs in the dyes support that the transitions at maximum absorptions have intramolecular CT (IMCT) character. So the transitions are not pure CT excitations, which can form complete charge separated states. The further MO analysis indicates that the coumarin, DMA, and aniline groups are effective chromophores in IMCT, and then they play important role in the sensitization of DSC. Also, the dyes with higher J_{sc} have more excited states with IMCT character in UV–vis region. For instance, for NKX-2883, five excited states with larger oscillator strength in UV–vis region have IMCT character, and the 16.9 mA/cm^2 J_{sc} is largest in these dyes. Similarly, NKX-2311 and NKX-2753 have more CT excited states with larger oscillator strength, and the J_{sc} of the dyes (15.2 and 16.1 mA/cm^2) are larger. More CT excited states in UV–vis region, which relate to the higher density of states near Fermi level [88], are favorable to harvest solar radiation. As to NKX-2195, the loss of planarity between conjugate bridge and anchor group reduce the electron injection rate and J_{sc} (7.5 mA/cm^2). With the increasing of alkenyl chain length (from C343, NKX-2388, to NKX-2311), the corresponding λ_{max} (390, 475, 495 nm, respectively) has a red-shift which is expected to match the solar radiation spectra. The corresponding oscillator strength (0.6392, 1.0571, 1.5531) also increases in the order because the longer conjugate bridge extends the overlap of HOMO and LUMO. The larger oscillator strength generates shorter lifetime of excited CT states, and thus fast CT and larger J_{sc}. So, the increasing for the length of alkenyl chain generates larger oscillator strength which induces fast CT and larger J_{sc}.

4. Conclusions

The geometries, electronic structures, dipole moments and polarizabilities for organic dye sensitizers C343 and NKX derivatives were calculated using DFT, and the electronic absorption properties were investigated using TD-DFT. Generally, the present theoretical results agree with the available experimental results and the reported theoretical works. Based upon the theoretical calculations and the reported experimental results of dye sensitizers and DSC, we can find the followings:

(1) The geometrical characters of dye sensitizers with good performance in DSC indicate that the planar conjugation from π-conjugate bridge to the acceptor group is favorable to improve the performance, and the appropriate conjugate length of dye sensitizer is also very important to increase the PCCE.
(2) The population analysis suggests that the charges of similar acceptors in different dyes are very similar, but the charges of donors and conjugate bridges are more flexible. Introducing strong electronic pull group in acceptor of dye sensitizer may generate larger electric potential barrier, and it is possible to increase the V_{oc} of DSC.
(3) The longer alkenyl and thiophene chain in conjugate bridge result in the higher HOMO energy, and then induce smaller driving force for the reduction of oxidized dyes. Whereas, the introducing strong pull-electron groups in acceptor stabilize the HOMO and LUMO, and reduce the E_g. So it may increase the driving force for the reduction of the oxidized dyes. The orbital energies disclose that the interfical electron transfer from dye sensitizer NKX derivatives to TiO_2 is an electron injection process.
(4) The dyes with larger polarizabilities possess the larger dipole moments because the longer conjugate bridge enhanced the electron delocalization. Elongating the conjugate bridge using alkenyl and introducing strong pull-electron group in the acceptor generate larger dipole moment, and tune the up-shift of valence and conduction bands of TiO_2. Thus, it may affect on the V_{oc} of DSC.
(5) The absorption properties and MO analysis indicate that the coumarin, DMA, and aniline groups are effective chromophores in IMCT, and they play an important role in sensitization of DSC. Also, the dyes with higher J_{sc} have more excited states with CT character in UV–vis region, and the increasing for the length of alkenyl chain generates larger oscillator strength, fast CT and larger J_{sc}.

Acknowledgements

This work supported by National Science Foundation of China (Grant Nos. 11164016, 11164015), the Basic Scientific Research Foundation for Gansu Universities of China, and Scientific Developmental Foundation of Lanzhou University of Technology.

Appendix A. Supplementary data

Supplementary data associated with this article can be found, in the online version, at http://dx.doi.org/10.1016/j.jmgm.2012.09.004.

References

[1] B. Oregan, M. Gratzel, A low-cost high-efficiency solar-cell based on dye-sensitized colloidal TiO_2 films, Nature 353 (1991) 737–740.
[2] M. Gratzel, Photoelectrochemical cells, Nature 414 (2001) 338–344.
[3] M. Gratzel, Dye-sensitized solar cells, Journal of Photochemistry and Photobiology C 4 (2003) 145–153.
[4] M.K. Nazeeruddin, C. Klein, P. Liska, M. Gratzel, Synthesis of novel ruthenium sensitizers and their application in dye-sensitized solar cells, Coordination Chemical Reviews 249 (2005) 1460–1467.
[5] B. Li, L. Wang, B. Kang, P. Wang, Y. Qiu, Review of recent progress in solid-state dye-sensitized solar cells, Solar Energy Materials and Solar Cells 90 (2006) 549–573.
[6] M. Gratzel, Recent advances in sensitized mesoscopic solar cells, Accounts of Chemical Research 42 (2009) 1788–1798.

[7] A. Mishra, M.K.R. Fischer, P. Bauerle, Metal-free organic dyes for dye-sensitized solar cells: from structure: property relationships to design rules, Angewandte Chemie International Edition 48 (2009) 2474–2499.
[8] Z.J. Ning, H. Tian, Triarylamine: a promising core unit for efficient photovoltaic materials, Chemical Communications (2009) 5483–5495.
[9] N. Robertson, Optimizing dyes for dye-sensitized solar cells, Angewandte Chemie International Edition 45 (2006) 2338–2345.
[10] S.M. Zakeeruddin, M. Gratzel, Solvent-free ionic liquid electrolytes for mesoscopic dye-sensitized solar cells, Advanced Functional Materials 19 (2009) 2187–2202.
[11] J.N. Clifford, E. Martinez-Ferrero, A. Viterisi, E. Palomares, Sensitizer molecular structure-device efficiency relationship in dye sensitized solar cells, Chemical Society Reviews 40 (2011) 1635–1646.
[12] M. Gratzel, Solar energy conversion by dye-sensitized photovoltaic cells, Inorganic Chemistry 44 (2005) 6841–6851.
[13] M.K. Nazeeruddin, A. Kay, I. Rodicio, R. Humphrybaker, E. Muller, P. Liska, N.M. Vlachopoulos, Gratzel. conversion of light to electricity by cis-X_2bis(2,2′-bipyridyl-4,4′-dicarboxylate)ruthenium(II) charge-transfer sensitizers (X = Cl^-, Br^-, I^-, CN^-, and SCN^-) on nanocrystalline TiO_2 electrodes, Journal of the American Ceramic Society 115 (1993) 6382–6390.
[14] M.K. Nazeeruddin, P. Pechy, T. Renouard, S.M. Zakeeruddin, R. Humphry-Baker, P. Comte, P. Liska, L. Cevey, E. Costa, V. Shklover, L. Spiccia, G.B. Deacon, C.A. Bignozzi, M. Gratzel, Engineering of efficient panchromatic sensitizers for nanocrystalline TiO_2-based solar cells, Journal of the American Chemical Society 123 (2001) 1613–1624.
[15] X.Y. Chen, J.H. Guo, X.J. Peng, M. Guo, Y.Q. Xu, L. Shi, C.L. Liang, L. Wang, Y.L. Gao, S.G. Sun, S.M. Cai, Novel cyanine dyes with different methine chains as sensitizers for nanocrystalline solar cell, Journal of Photochemistry and Photobiology A 171 (2005) 231–236.
[16] K. Sayama, S. Tsukagoshi, T. Mori, K. Hara, Y. Ohga, A. Shinpou, Y. Abe, S. Suga, H. Arakawa, Efficient sensitization of nanocrystalline TiO_2 films with cyanine and merocyanine organic dyes, Solar Energy Materials and Solar Cells 80 (2003) 47–71.
[17] W.J. Wu, J.L. Hua, Y.H. Jin, W.H. Zhan, H. Tian, Photovoltaic properties of three new cyanine dyes for dye-sensitized solar cells, Photochemistry and Photobiology Science 7 (2008) 63–68.
[18] Y.S. Chen, C. Li, Z.H. Zeng, W.B. Wang, X.S. Wang, B.W. Zhang, Efficient electron injection due to a special adsorbing group's combination of carboxyl and hydroxyl: dye-sensitized solar cells based on new hemicyanine dyes, Journal of Materials Chemistry 15 (2005) 1654–1661.
[19] Z.S. Wang, F.Y. Li, C.H. Huang, Photocurrent enhancement of hemicyanine dyes containing RSO_3^- group through treating TiO_2 films with hydrochloric acid, Journal of Physical Chemistry B 105 (2001) 9210–9217.
[20] M. Liang, W. Xu, F.S. Cai, P.Q. Chen, B. Peng, J. Chen, Z.M. Li, New triphenylamine-based organic dyes for efficient dye-sensitized solar cells, Journal of Physical Chemistry C 111 (2007) 4465–4472.
[21] P. Shen, Y.H. Tang, S.H. Jiang, H.J. Chen, X.Y. Zheng, X.Y. Wang, B. Zhao, S.T. Tan, Efficient triphenylamine-based dyes featuring dual-role carbazole fluorene and spirobifluorene moieties, Organic Electronics 12 (2011) 125–135.
[22] U.B. Cappel, M.H. Karlsson, N.G. Pschirer, F. Eickemeyer, J. Schoneboom, P. Erk, G. Boschloo, A. Hagfeldt, A broadly absorbing perylene dye for solid-state dye-sensitized solar cells, Journal of Physical Chemistry C 113 (2009) 14595–14597.
[23] C.J. Jiao, N.N. Zu, K.W. Huang, P. Wang, J.S. Wu, Perylene anhydride fused porphyrins as near-infrared sensitizers for dye-sensitized solar cells, Organic Letters 13 (2011) 3652–3655.
[24] C. Li, J. Schoneboom, Z.H. Liu, N.G. Pschirer, P. Erk, A. Herrmann, K. Mullen, Rainbow perylene monoimides: easy control of optical properties, Chemistry: A European Journal 15 (2009) 878–884.
[25] C. Li, J.H. Yum, S.J. Moon, A. Herrmann, F. Eickemeyer, N.G. Pschirer, P. Erk, J. Schoeboom, K. Mullen, M. Gratzel, M.K. Nazeeruddin, An improved perylene sensitizer for solar cell applications, Chemsuschem 1 (2008) 615–618.
[26] H. Tian, P.H. Liu, W.H. Zhu, E.Q. Gao, W.A. Da-Jun, S.M. Cai, Synthesis of novel multi-chromophoric soluble perylene derivatives and their photosensitizing properties with wide spectral response for SnO_2 nanoporous electrode, Journal of Materials Chemistry 10 (2000) 2708–2715.
[27] K. Hara, T. Sato, R. Katoh, A. Furube, Y. Ohga, A. Shinpo, S. Suga, K. Sayama, H. Sugihara, H. Arakawa, Molecular design of coumarin dyes for efficient dye-sensitized solar cells, Journal of Physical Chemistry B 107 (2003) 597–606.
[28] S.E. Koops, P.R.F. Barnes, B.C. O'Regan, J.R. Durrant, Kinetic competition in a coumarin dye-sensitized solar cell: injection and recombination limitations upon device performance, Journal of Physical Chemistry C 114 (2010) 8054–8061.
[29] X.G. Li, H.J. Lu, S.R. Wang, J.J. Guo, J. Li, Sensitizers of dye-sensitized solar cells, Progress in Chemistry 23 (2011) 569–588.
[30] W.M. Campbell, A.K. Burrell, D.L. Officer, K.W. Jolley, Porphyrins as light harvesters in the dye-sensitised TiO_2 solar cell, Coordination Chemistry Reviews 248 (2004) 1363–1379.
[31] C.P. Hsieh, H.P. Lu, C.L. Chiu, C.W. Lee, S.H. Chuang, C.L. Mai, W.N. Yen, S.J. Hsu, E.W.G. Diau, C.Y. Yeh, Synthesis and characterization of porphyrin sensitizers with various electron-donating substituents for highly efficient dye-sensitized solar cells, Journal of Materials Chemistry 20 (2010) 1127–1134.
[32] H. Imahori, T. Umeyama, S. Ito, Large π-aromatic molecules as potential sensitizers for highly efficient dye-sensitized solar cells, Accounts of Chemical Research 42 (2009) 1809–1818.
[33] C.W. Lee, H.P. Lu, C.M. Lan, Y.L. Huang, Y.R. Liang, W.N. Yen, Y.C. Liu, Y.S. Lin, E.W.G. Diau, C.Y. Yeh, Novel zinc porphyrin sensitizers for dye-sensitized solar cells: synthesis and spectral electrochemical, and photovoltaic properties, Chemistry: A European Journal 15 (2009) 1403–1412.
[34] K.K. Pasunooti, J.L. Song, H. Chai, P. Amaladass, W.Q. Deng, X.W. Liu, Synthesis characterization and application of trans-D-π-A-porphyrin based dyes in dye-sensitized solar cells, Journal of Photochemistry and Photobiology A 218 (2011) 219–225.
[35] S.L. Wu, H.P. Lu, H.T. Yu, S.H. Chuang, C.L. Chiu, C.W. Lee, E.W.G. Diau, C.Y. Yeh, Design and characterization of porphyrin sensitizers with a push–pull framework for highly efficient dye-sensitized solar cells, Energy & Environment Science 3 (2010) 949–955.
[36] T. Geiger, S. Kuster, J.H. Yum, S.J. Moon, M.K. Nazeeruddin, M. Gratzel, F. Nuesch, Molecular design of unsymmetrical squaraine dyes for high efficiency conversion of low energy photons into electrons using TiO_2 nanocrystalline films, Advanced Functional Materials 19 (2009) 2720–2727.
[37] S. Paek, H. Choi, C. Kim, N. Cho, S. So, K. Song, M.K. Nazeeruddin, J. Ko, Efficient and stable panchromatic squaraine dyes for dye-sensitized solar cells, Chemical Communications 47 (2011) 2874–2876.
[38] F. Silvestri, I. Lopez-Duarte, W. Seitz, L. Beverina, M.V. Martinez-Diaz, T.J. Marks, D.M. Guldi, G.A. Pagani, T. Torres, A squaraine–phthalocyanine ensemble: towards molecular panchromatic sensitizers in solar cells, Chemical Communications (2009) 4500–4502.
[39] H.M. Cheng, W.F. Hsieh, Electron transfer properties of organic dye-sensitized solar cells based on indoline sensitizers with ZnO nanoparticles, Nanotechnology 21 (2010) 485202.
[40] D. Kuang, S. Uchida, R. Humphry-Baker, S.M. Zakeeruddin, M. Gratzel, Organic dye-sensitized ionic liquid based solar cells: remarkable enhancement in performance through molecular design of indoline sensitizers, Angewandte Chemie International Edition 47 (2008) 1923–1927.
[41] X.H. Zhang, C. Li, W.B. Wang, X.X. Cheng, X.S. Wang, B.W. Zhang, Photophysical, electrochemical and photoelectrochemical properties of new azulene-based dye molecules, Journal of Materials Chemistry 17 (2007) 642–649.
[42] W.D. Zeng, Y.M. Cao, Y. Bai, Y.H. Wang, Y.S. Shi, M. Zhang, F.F. Wang, C.Y. Pan, P. Wang, Efficient dye-sensitized solar cells with an organic photosensitizer featuring orderly conjugated ethylenedioxythiophene and dithienosilole blocks, Chemistry of Materials 22 (2010) 1915–1925.
[43] J.M. Rehm, G.L. McLendon, Y. Nagasawa, K. Yoshihara, J. Moser, M. Gratzel, Femtosecond electron-transfer dynamics at a sensitizing dye–semiconductor TiO_2 interface, Journal of Physical Chemistry 100 (1996) 9577–9578.
[44] K. Hara, K. Sayama, Y. Ohga, A. Shinpo, S. Suga, H. Arakawa, A coumarin-derivative dye sensitized nanocrystalline TiO_2 solar cell having a high solar-energy conversion efficiency up to 5.6%, Chemical Communications (2001) 569–570.
[45] K. Hara, Y. Tachibana, Y. Ohga, A. Shinpo, S. Suga, K. Sayama, H. Sugihara, H. Arakawa, Dye-sensitized nanocrystalline TiO_2 solar cells based on novel coumarin dyes, Solar Energy Materials and Solar Cells 77 (2003) 89–103.
[46] K. Hara, M. Kurashige, Y. Dan-oh, C. Kasada, A. Shinpo, S. Suga, K. Sayama, H. Arakawa, Design of new coumarin dyes having thiophene moieties for highly efficient organic-dye-sensitized solar cells, New Journal of Chemistry 27 (2003) 783–785.
[47] K. Hara, Z.S. Wang, T. Sato, A. Furube, R. Katoh, H. Sugihara, Y. Dan-Oh, C. Kasada, A. Shinpo, S. Suga, Oligothiophene-containing coumarin dyes for efficient dye-sensitized solar cells, Journal of Physical Chemistry B 109 (2005) 15476–15482.
[48] Z.S. Wang, Y. Cui, Y. Dan-Oh, C. Kasada, A. Shinpo, K. Hara, Thiophene-functionalized coumarin dye for efficient dye-sensitized solar cells: electron lifetime improved by coadsorption of deoxycholic acid, Journal of Physical Chemistry C 111 (2007) 7224–7230.
[49] Z.S. Wang, Y. Cui, K. Hara, Y. Dan-Oh, C. Kasada, A. Shinpo, A high-light-harvesting-efficiency coumarin dye for stable dye-sensitized solar cells, Advanced Materials 19 (2007) 1138–1141.
[50] Z.S. Wang, Y. Cui, Y. Dan-Oh, C. Kasada, A. Shinpo, K. Hara, Molecular design of coumarin dyes for stable and efficient organic dye-sensitized solar cells, Journal of Physical Chemistry C 112 (2008) 17011–17017.
[51] Z.S. Wang, K. Hara, Y. Dan-Oh, C. Kasada, A. Shinpo, S. Suga, H. Arakawa, H. Sugihara, Photophysical and (photo)electrochemical properties of a coutnarin dye, Journal of Physical Chemistry B 109 (2005) 3907–3914.
[52] K. Hara, M. Kurashige, S. Ito, A. Shinpo, S. Suga, K. Sayama, H. Arakawa, Novel polyene dyes for highly efficient dye-sensitized solar cells, Chemical Communications (2003) 252–253.
[53] K. Hara, T. Sato, R. Katoh, A. Furube, T. Yoshihara, M. Murai, M. Kurashige, S. Ito, A. Shinpo, S. Suga, H. Arakawa, Novel conjugated organic dyes for efficient dye-sensitized solar cells, Advanced Functional Materials 15 (2005) 246–252.
[54] C.-K. Tai, Y.-J. Chen, H.-W. Chang, P.-L. Yeh, B.-C. Wang, DFT and TD-DFT investigations of metal-free dye sensitizers for solar cells: effects of electron donors and -conjugated linker, Computational and Theoretical Chemistry 971 (2011) 42–50.
[55] B.-G. Kim, C.-G. Zhen, E.J. Jeong, J. Kieffer, J. Kim, Organic dye design tools for efficient photocurrent generation in dye-sensitized solar cells: exciton binding energy and electron acceptors, Advanced Functional Materials 22 (2012) 1606–1612.
[56] Y. Kurashige, T. Nakajima, S. Kurashige, K. Hirao, Y. Nishikitani, Theoretical investigation of the excited states of coumarin dyes for dye-sensitized solar cells, Journal of Physical Chemistry A 111 (2007) 5544–5548.
[57] X. Zhang, J.J. Zhang, Y.Y. Xia, Molecular design of coumarin dyes with high efficiency in dye-sensitized solar cells, Journal of Photochemistry and Photobiology A 194 (2008) 167–172.

[58] M.M. Waskasi, S.M. Hashemianzadeh, O.M. Sarhangi, Significant enhancement in efficiency of NKX-2807 coumarin dye by applying external electric field in dye sensitizer solar cell: theoretical study, Computational and Theoretical Chemistry 978 (2011) 33–40.
[59] A.D. Becke, density-functional exchange-energy approximation with correct asymptotic-behavior, Physical Review A 38 (1988) 3098–3100.
[60] A.D. Becke, Density-functional thermochemistry. 3. The role of exact exchange, Journal of Chemical Physics 98 (1993) 5648–5652.
[61] C.T. Lee, W.T. Yang, R.G. Parr, development of the Colle–Salvetti correlation-energy formula into a functional of the electron-density, Physical Review B 37 (1988) 785–789.
[62] M.J. Frisch, G.W. Trucks, H.B. Schlegel, G.E. Scuseria, M.A. Robb, J.R. Cheeseman, J.A. Montgomery, T.V. Jr., K.N. Kudin, J.C. Burant, J.M. Millam, S.S. Iyengar, J. Tomasi, V. Barone, B. Mennucci, M. Cossi, G. Scalmani, N. Rega, G.A. Petersson, H. Nakatsuji, M. Hada, M. Ehara, K. Toyota, R. Fukuda, J. Hasegawa, M. Ishida, T. Nakajima, Y. Honda, O. Kitao, H. Nakai, M. Klene, X. Li, J.E. Knox, H.P. Hratchian, J.B. Cross, C. Adamo, J. Jaramillo, R. Gomperts, R.E. Stratmann, O. Yazyev, A.J. Austin, R. Cammi, C. Pomelli, J.W. Ochterski, P.Y. Ayala, K. Morokuma, G.A. Voth, P. Salvador, J.J. Dannenberg, V.G. Zakrzewski, S. Dapprich, A.D. Daniels, M.C. Strain, O. Farkas, D.K. Malick, A.D. Rabuck, K. Raghavachari, J.B. Foresman, J.V. Ortiz, Q. Cui, A.G. Baboul, S. Clifford, J. Cioslowski, B.B. Stefanov, G. Liu, A. Liashenko, P. Piskorz, I. Komaromi, R.L. Martin, D.J. Fox, T. Keith, M.A. Al-Laham, C.Y. Peng, A. Nanayakkara, M. Challacombe, P.M.W. Gill, B. Johnson, W. Chen, M.W. Wong, C. Gonzalez, J.A. Pople, Gaussian 03, Gaussian Inc., Wallingford, CT, 2004.
[63] M. Pastore, E. Mosconi, F. De Angelis, M. Gratzel., A computational investigation of organic dyes for dye-sensitized solar cells: benchmark, strategies, and open issues, Journal of Physical Chemistry C 114 (2010) 7205–7212.
[64] C. Adamo, V. Barone, Toward reliable density functional methods without adjustable parameters: the PBE0 model, Journal of Chemical Physics 110 (1999) 6158–6170.
[65] O.A. Vydrov, G.E. Scuseria, J.P. Perdew, Tests of functionals for systems with fractional electron number, Journal of Chemical Physics 126 (2007) 154109.
[66] O.A. Vydrov, G.E. Scuseria, Assessment of a long-range corrected hybrid functional, Journal of Chemical Physics 125 (2006) 234109.
[67] O.A. Vydrov, J. Heyd, A.V. Krukau, G.E. Scuseria, Importance of short-range versus long-range Hartree–Fock exchange for the performance of hybrid density functionals, Journal of Chemical Physics 125 (2006) 074106.
[68] Y. Tawada, T. Tsuneda, S. Yanagisawa, T. Yanai, K. Hirao, A long-range-corrected time-dependent density functional theory, Journal of Chemical Physics 120 (2004) 8425–8433.
[69] M.J. Frisch, G.W. Trucks, H.B. Schlegel, G.E. Scuseria, M.A. Robb, J.R. Cheeseman, G. Scalmani, V. Barone, B. Mennucci, G.A. Petersson, H. Nakatsuji, M. Caricato, X. Li, H.P. Hratchian, A.F. Lzmaylov, J. Bloino, G. Zheng, J.L. Sonnenberg, M. Hada, M. Ehara, K. Toyota, R. Fukuda, J. Hasegawa, M. Ishida, T. Nakajima, Y. Honda, O. Kitao, H. Nakai, T. Vreven, M. J.A Jr., J.E. Peralta, F. Ogliaro, M. Bearpark, J.J. Heyd, E. Brothers, K.N. Kudin, V.N. Staroverov, T. Keith, R. Kobayashi, J. Normand, K. Raghavachari, A. Rendell, J.C. Burant, S.S. Lyengar, J. Tomasi, M. Cossi, N. Rega, J.M. Millam, M. Klene, J.E. Knox, J.B. Cross, V. Bakken, C. Adamo, J. Jaramillo, R. Gomperts, R.E. Stratmann, O. Yazyev, A.J. Austin, R. Cammi, C. Pomelli, J.W. Ochterski, R.L. Martin, K. Morokuma, V.G. Zakrzewski, G.A. Voth, P. Salvador, J.J. Dannenberg, S. Dapprich, A.D. Daniels, O. Farkas, J.B. Foresman, J.V. Ortiz, J. Cioslowski, D.J. Fox, Gaussian09, Gaussian Inc., Wallingford, CT, 2010.
[70] J. Tomasi, B. Mennucci, R. Cammi, Quantum mechanical continuum solvation models, Chemical Reviews 105 (2005) 2999–3093.
[71] S.I. Gorelsky, SWizard program, <http://www.sg-chem.net>.
[72] S. Kim, J.K. Lee, S.O. Kang, J. Ko, J.H. Yum, S. Fantacci, F. De Angelis, D. Di Censo, M.K. Nazeeruddin, M. Gratzel, Molecular engineering of organic sensitizers for solar cell applications, Journal of the American Chemical Society 128 (2006) 16701–16707.
[73] C.R. Zhang, Y.Z. Wu, Y.H. Chen, H.S. Chen Geometries, electronic structures and related properties of organic dye sensitizers JK16 and JK17, Acta Physico-Chimica Sinica 25 (2009) 53–60.
[74] H. Choi, J.K. Lee, K. Song, S.O. Kang, J. Ko, Novel organic dyes containing bis-dimethylfluorenyl amino benzo[*b*]thiophene for highly efficient dye-sensitized solar cell, Tetrahedron 63 (2007) 3115–3121.
[75] C.R. Zhang, Z.J. Liu, Y.H. Chen, H.S. Chen, Y.Z. Wu, L.H. Yuan, DFT and TDDFT study on organic dye sensitizers D5 DST and DSS for solar cells, Journal of Molecular Structure (Theochem) 899 (2009) 86–93.
[76] C.R. Zhang, Z.J. Liu, Y.H. Chen, H.S. Chen, Y.Z. Wu, W.J. Feng, D.B. Wang, DFT and TD-DFT study on structure and properties of organic dye sensitizer TA-St-CA, Current Applied Physics 10 (2010) 77–83.
[77] I. Jung, J.K. Lee, K.H. Song, K. Song, S.O. Kang, J. Ko, Synthesis and photovoltaic properties of efficient organic dyes containing the benzo[*b*]furan moiety for solar cells, Journal of Organic Chemistry 72 (2007) 3652–3658.
[78] D. Casanova, The role of the π linker in donor-π-acceptor organic dyes for high-performance sensitized solar cells, Chemphyschem 12 (2011) 2979–2988.
[79] O. Christiansen, J. Gauss, J.F. Stanton, Frequency-dependent polarizabilities and first hyperpolarizabilities of CO and H_2O from coupled cluster calculations, Chemical Physics Letters 305 (1999) 147–155.
[80] Z.S. Wang, Y.Y. Huang, C.H. Huang, J. Zheng, H.M. Cheng, S.J. Tian, Photosensitization of ITO and nanocrystalline TiO_2 electrode with a hemicyanine derivative, Synthetic Metals 114 (2000) 201–207.
[81] F. De Angelis, S. Fantacci, A. Selloni, M. Gratzel, M.K. Nazeeruddin, Influence of the sensitizer adsorption mode on the open-circuit potential of dye-sensitized solar cells, Nano Letters 7 (2007) 3189–3195.
[82] J. Preat, C. Michaux, D. Jacquemin, E.A. Perpéte., Enhanced efficiency of organic dye-sensitized solar cells: triphenylamine derivatives, Journal of Physical Chemistry C 113 (2009) 16821–16833.
[83] W. Fan, D. Tan, W. Deng, Theoretical investigation of triphenylamine dye/titanium dioxide interface for dye-sensitized solar cells, Physical Chemistry Chemical Physics 13 (2011) 16159–16167.
[84] W. Fan, D. Tan, W.-Q. Deng, Acene-modified triphenylamine dyes for dye-sensitized solar cells: a computational study, ChemPhysChem 13 (2012) 2051–2060.
[85] R. Baer, E. Livshits, U. Salzner, Tuned range-separated hybrids in density functional theory, Annual Review of Physical Chemistry 61 (2010) 85–109.
[86] D. Jacquemin, E.A. Perpéte, I. Ciofini, C. Adamo, Accurate simulation of optical properties in dyes, Accounts of Chemical Research 42 (2009) 326–334.
[87] S.S. Leang, F. Zahariev, M.S. Gordon, Benchmarking the performance of time-dependent density functional methods, Journal of Chemical Physics 136 (2012) 104101.
[88] C.R. Zhang, Z.J. Liu, Y.T. Sun, Y.L. Shen, Y.H. Chen, Y.J. Liu, W. Wang, H.M. Zhang, Electronic structures and absorption properties of three kinds of ruthenium dye sensitizers containing bipyridine-pyrazolate for solar cells, Spectrochimica Acta Part A 79 (2011) 1843–1848.